

# 9.)

## Industrial, analytical, and medical applications. (Lilley Chap.8 and 9)

### Industrial use

- 1.) Tracer-based measurements (incorporation in biological systems, measuring abrasion and leaks)
- 2.) Thickness measurements, level measurements.
- 3.) Material modifications (hardening and shrinking)
- 4.) Food sterilization (spice)
- 5.) Industrial radiography (welding inspection)

### Neutron activation analysis

- 1.) This is an alternative solution to the regular tracer techniques. Only the samples collected are made radioactive.
- 2.) Deciding the amount of unknown elements in a sample.

Induced activity:  $A(t) = \lambda n(t) = \dot{\Phi}\sigma \cdot N_{target}[1 - e^{-\lambda t}]$  for  $\dot{\Phi}\sigma \ll \lambda$

$$\frac{dN_{target}}{dt} = -\dot{\Phi}\sigma N_{target}$$

$$\frac{dn}{dt} = \dot{\Phi}\sigma N_{target} - \lambda \cdot n$$

$$\Rightarrow n(t) = \frac{\dot{\Phi}\sigma \cdot N_{target}}{\lambda - \dot{\Phi}\sigma} [e^{-\dot{\Phi}\sigma t} - e^{-\lambda t}]$$

## Rutherford backscattering

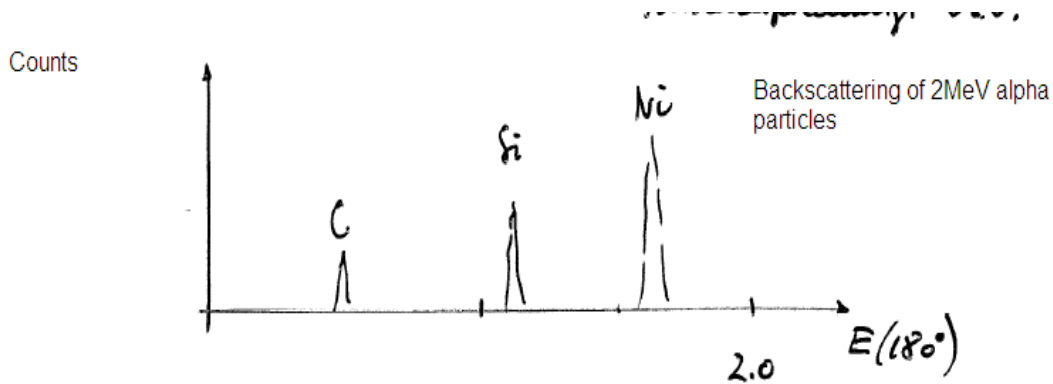
Rutherford scattering cross-section in the lab system for  $M < \infty$  ( $M \rightarrow \infty$  makes the lab and CM systems equivalent):

$$\text{Rutherford cross-section: } \frac{d\sigma_R}{d\Omega} = 1.296 \left[ \frac{zZ}{E_0} \right]^2 \left[ \frac{1}{\sin^4 \frac{\psi}{2}} - \left( \frac{m}{M} \right)^2 + \dots \right] \frac{mb}{sr}$$

Where  $\psi$  is the scattering angle in the lab system. The energy of the particle ( $m$ ) backscattered from the target ( $M$ ):

$$\text{Particle energy: } E(\pi) = \left[ \frac{M-m}{M+m} \right]^2 E_0$$

$E_0$  is the particle energy immediately before interacting with the target (energy loss along particle track).

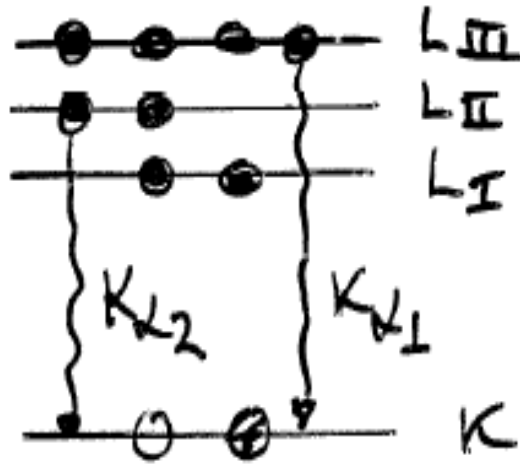


In "thick" samples, the particle energy is degraded both before and after backscattering. The method is ideal to detect occurrence of heavy elements in a material consisting of light elements.

## Particle-induced X-ray emission (PIXE)

This method is particularly sensitive when it comes to finding elements. The sensitivity is 0.1ppm, i.e. 1000 times better than the usual method of X-ray microanalysis by electron microscopy. Both identification and quantification based on excitation of characteristic X-ray radiation.

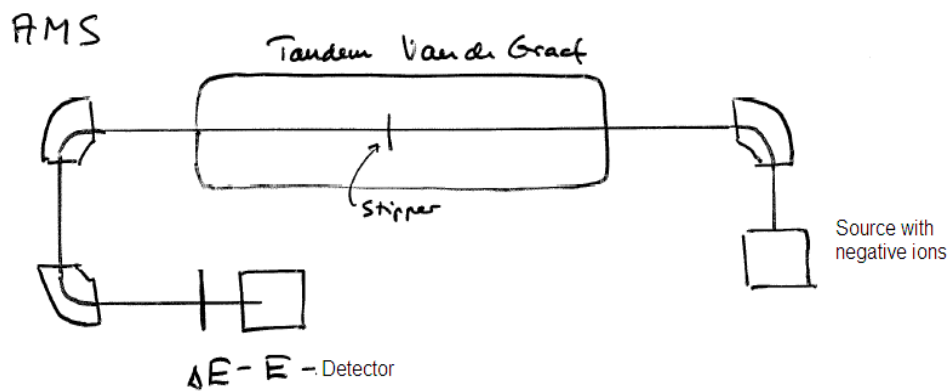
$$\text{X-ray production rate: } R_X = \dot{\Phi} \cdot \sigma_x \cdot \underbrace{\frac{n_T}{V_T}}_{\#T/V_T} \cdot \underbrace{Adx}_{V_{Target}}$$



$L_I \rightarrow K$  is optically forbidden.

### Accelerator-based mass spectroscopy

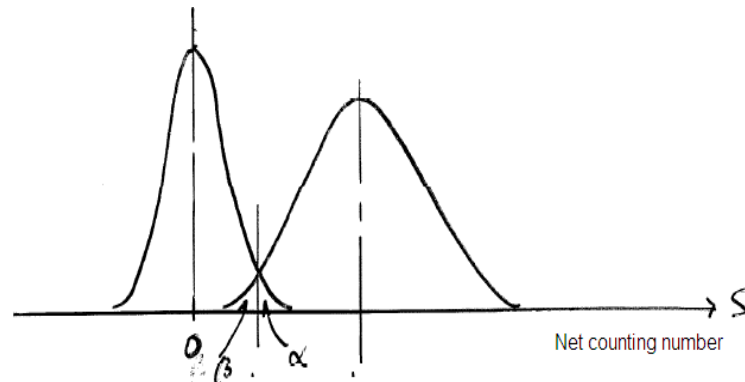
This is a sensitive method for counting  $^{14}\text{C}$ . This makes it ideal for carbon dating of biological materials. What makes this method so effective is that it counts all the  $^{14}\text{C}$  atoms in the sample, while radioactivity-based counting only counts a fraction  $\lambda \cdot T \ll 1$  during the time interval  $T$ . ( $\lambda = \frac{\ln 2}{5730\text{yrs}}$  for  $^{14}\text{C}$ )



Deflector magnets :  $\vec{F} = q(\vec{v} \times \vec{B}) = m\vec{a} \Rightarrow r = \frac{mv}{qB}$

Deflector magnets:  $\vec{F} = q(\vec{v} \times \vec{B}) = m \cdot \vec{a} \Rightarrow r = \frac{mv}{qB}$

## Low-activity counting



Radioactivity is modelled as a Bernoulli process which is represented by a binomial distribution.

For  $N \gg 1$ ,  $p = \lambda t \ll 1$ , the Binomial distribution  $\simeq$  Poisson distribution  $\simeq$  Gaussian distribution. To keep it simple, one uses a Gaussian distribution as a statistical model, combined with the result from the Poisson distribution:

$$\text{Standard deviation: } \sqrt{\lambda t} = \sqrt{n}$$

$$\text{Net number of counts: } S = n_g - n_b$$

Where  $n_g$  is the gross counts and  $n_b$  is the number of counts due to background radiation. Both these numbers are counted during the same time interval  $t$ .

$$\text{Standard deviation: } \sigma_S = \sqrt{\sigma_{n_g}^2 + \sigma_{n_b}^2} = \sqrt{n_g + n_b} = \sqrt{S + 2n_b}$$

## Minimum significant activity

$$P(\text{Type I error}) = P(\text{false positive}) \leq \alpha \text{ for } S \leq L_C$$

$$\text{The sample has 0 activity } \Rightarrow \sigma_S = \sigma_0 = \sqrt{2n_b}, \quad (S \simeq 0)$$

$$P_0(S) = \frac{1}{\sqrt{2\pi}\sigma_0} \cdot e^{-\frac{S^2}{2\sigma_0^2}}$$

$$L_c = k_\alpha \cdot \sigma_0$$

Where  $\alpha$  represents an  $\alpha$ -fractile in the Gaussian distribution. For example  $\alpha = 0.05 \Rightarrow k_\alpha = 1.645$

## Minimum detectable true activity

P(Type II error)=P(false negative) $\leq \beta$  for  $S \geq L_d$

$$L_d = L_C + k_\beta \sigma_d = k_\alpha \sigma_0 + k_\beta \sigma_d$$

In this case,  $S$  is  $N(L_d, \sigma_d)$ .

$$\text{Variance: } \sigma_d^2 = S_d + 2n_b = L_d + \sigma_0^2$$

$$\Rightarrow [L_d - k_\alpha \sigma_0]^2 = k_\beta^2 \sigma_d^2 = k_\beta^2 [L_d + \sigma_0^2]$$

$$\Rightarrow L_d = \frac{k_\beta^2 + 2k_\alpha \sigma_0}{2} + \sqrt{\left[\frac{k_\beta^2 + 2k_\alpha \sigma_0}{2}\right]^2 + [k_\beta^2 - k_\alpha^2] \sigma_0^2}$$

$$1.) \quad k_\alpha = k_\beta = k \Rightarrow L_d = k^2 + 2k\sigma_0$$

$$2.) \quad k_\alpha \sigma_0 \gg k_\beta^2 \Rightarrow L_d = (k_\alpha + k_\beta) \sigma_0$$

| I                       | II   | III                        |
|-------------------------|--|----------------------------|
| $S < L_c$               | $L_c < S < L_d$  | $S > L_d$                  |
| No significant activity | Significant activity,<br>but P(false negative) $> \beta$ | Significant, true activity |

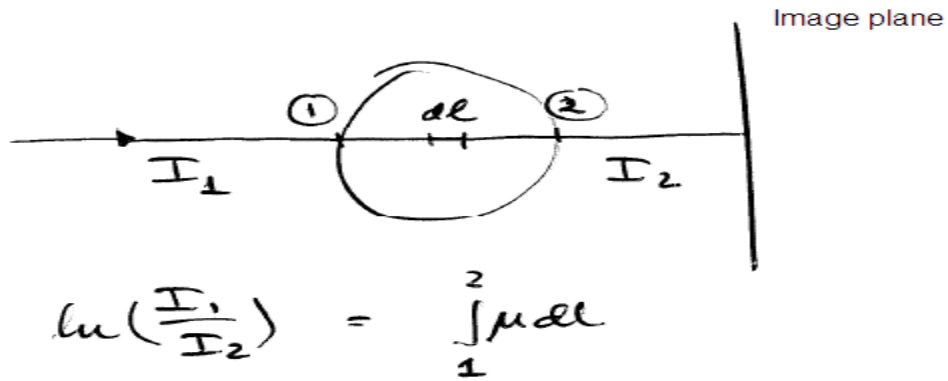
$$\text{Detection limits: } A_c = \frac{L_c}{\varepsilon \cdot T}, \quad A_d = \frac{L_d}{\varepsilon \cdot T}$$

During the time interval  $T$ , with an assumed counting efficiency  $\varepsilon$ .

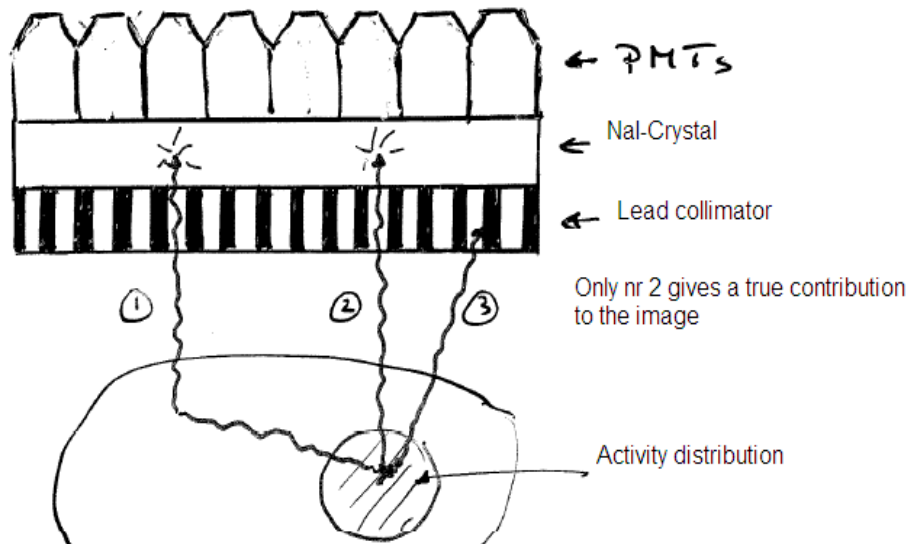
If the accurate background counting rate,  $r_b$  is known, the standard deviation:  $\sigma_0 = \sqrt{n_b} = \sqrt{B}$   
I.e,  $\sigma_{n_b} = 0$ ,  $B = r_b \cdot T$

## Nuclear imaging (Lilley chap 9)

Projection imaging (external source, conventional X-ray)



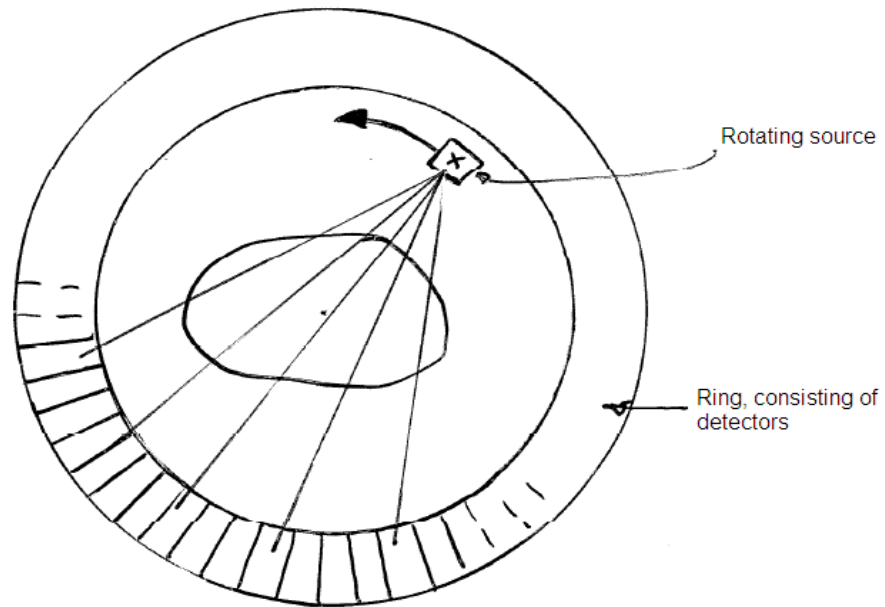
Internal source distribution imaged by a gamma camera



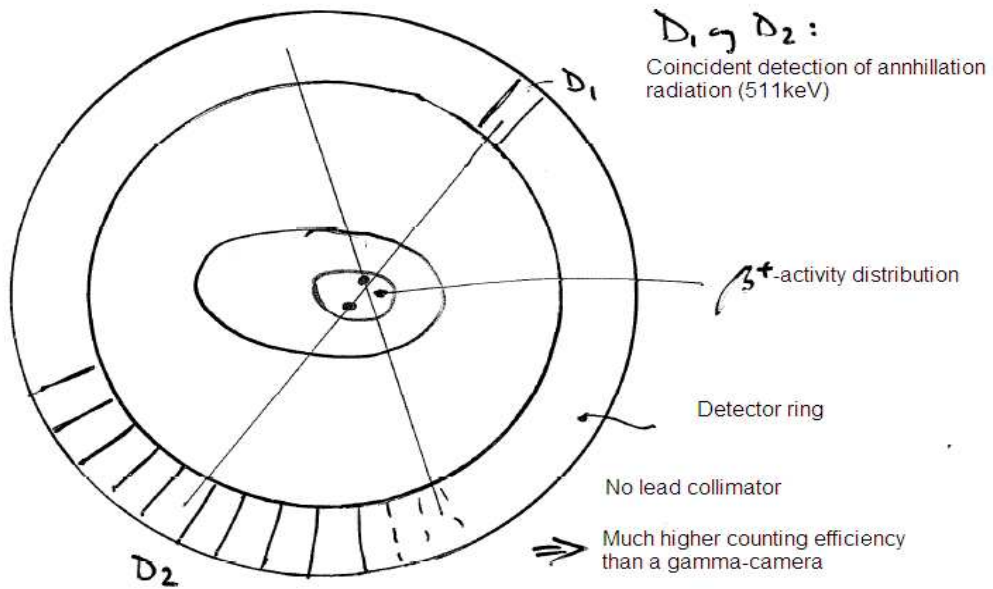
Projection imaging:  $X = \frac{\sum s_i x_i}{\sum s_i}$ ,  $Y = \frac{\sum s_i y_i}{\sum s_i}$ , where  $s_i$  is the signal in PMT  $i$ .

Energy discrimination:  $E = \sum s_i$  inside the full-energy peak.

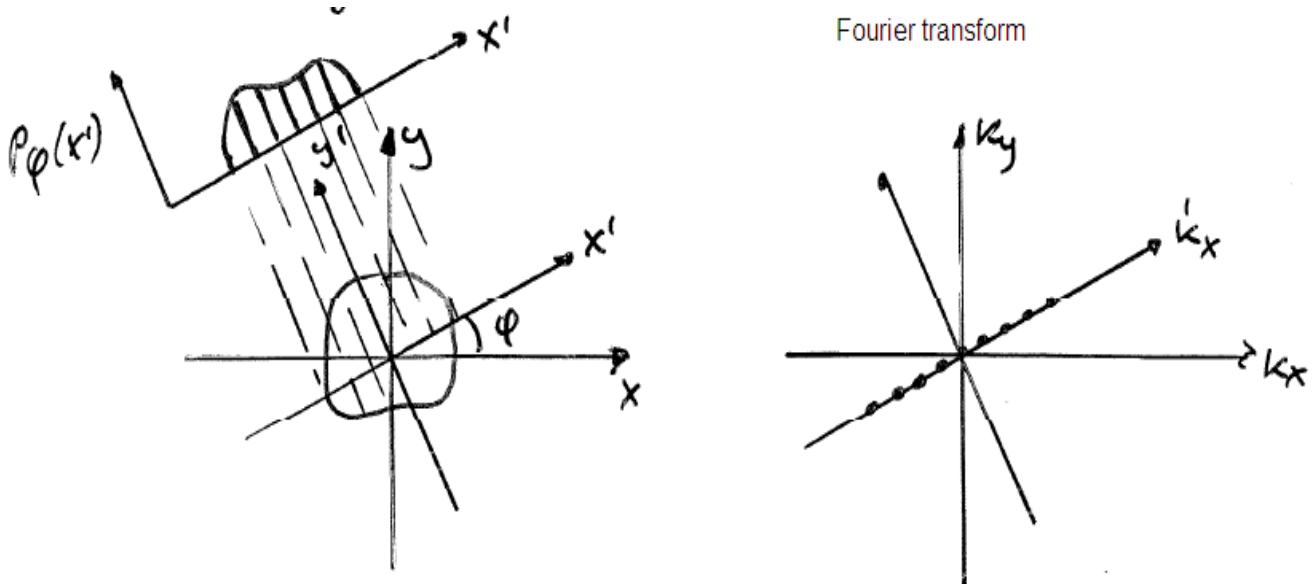
## X-ray CT (Computed Tomography)



## Positron Emission Tomography (PET)



## Filtered back-projection for reconstruction of images registered as a set of projection profiles

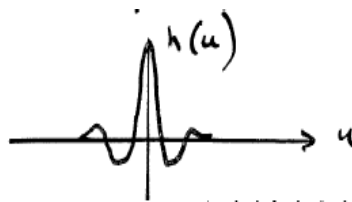


Central section theorem: The one-dimensional Fourier transform of the object's projection profile in the  $\phi$  direction, is equal to the central section of the two-dimensional Fourier transform of the object through the origin in the  $\phi$ -direction.  $\rightarrow M(k'_x, k'_y = 0) = M(k, \phi) = P_\phi(k'_x)$ , where  $M$  is the Fourier transform of the object and  $P_\phi$  is the Fourier transform of the profile in direction  $\phi$ .

$$\text{Filtered profile: } p_\phi^\dagger(x') = \mathcal{F}^{-1}[P_\phi(k) \cdot H(k)]$$

$$\text{Filter function: } H(k) = |k|$$

$$\Rightarrow p_\phi^\dagger(x') = \int_{-\infty}^{\infty} p_\phi(u) \cdot h(x' - u) du$$



$$\text{Filtered back-projection: } \mu(x, y) = \mathcal{F}^{-1}[M^P(k, \phi)] = \int_0^\phi p_\phi^\dagger(x') |_{x'=x\cos\phi+y\sin\phi} d\phi$$

Projection imaging results in averaging, which again leads to loss of high frequency information. Filtering with high frequency enhancement before image reconstruction by back-projection. Filtered back-projection can be used for SPECT, PET, X-ray CT, MR, etc.



## MR imaging

For all nuclei with spin  $I \neq 0$ .

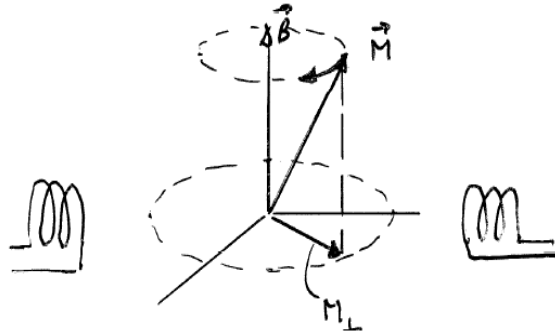
Mostly used for  $^1H$ -mapping.

Net magnetization:  $\vec{M} = \gamma \vec{L}$ ,  $\gamma = \frac{2\mu_p}{\hbar}$

$$M = \Delta N \cdot \mu_p$$

$$L = \Delta N \cdot S_z = \Delta N \cdot \frac{1}{2}\hbar$$

$$\Delta N = N_+ - N_- = N_+[1 - e^{-\frac{\Delta E}{kT}}] \simeq \frac{N}{2} \cdot \frac{2\mu_p B}{kT}, \quad \Delta E = 2\mu_p B$$



Precession of  $\vec{M}$  around the direction of the  $\vec{B}$ -field at the Larmor frequency  $\omega_L$ .

Torque:  $\frac{d\vec{L}}{dt} = \vec{M} \times \vec{B}$

$$\Rightarrow \omega_L = \frac{2\mu_p \cdot B}{\hbar} = \gamma B$$

Excitation field at Larmor frequency  $\omega_L$ :  $B_{ex}$  in the horizontal plane.  $\frac{B_{ex}}{2}$  is found to be a constant field in a rotating co-ordinate system, rotating at the Larmor frequency:  $\Rightarrow$  Precession around the  $x'$ -axis at the frequency  $\omega' = \frac{2\mu_p}{\hbar} \cdot \frac{B_{ex}}{2}$

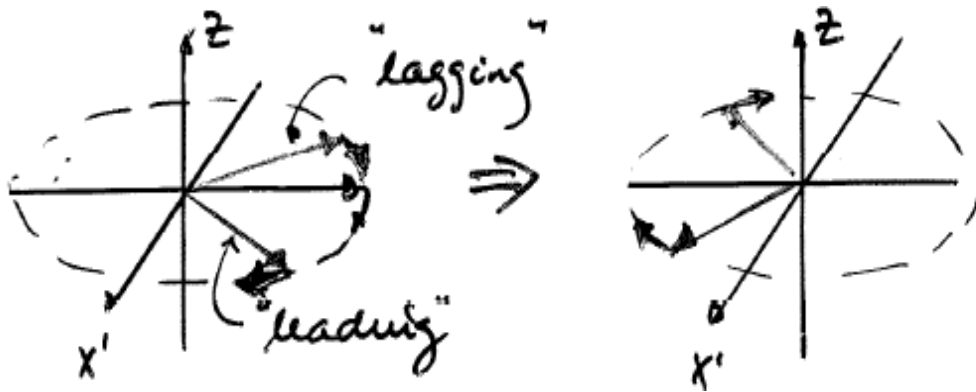
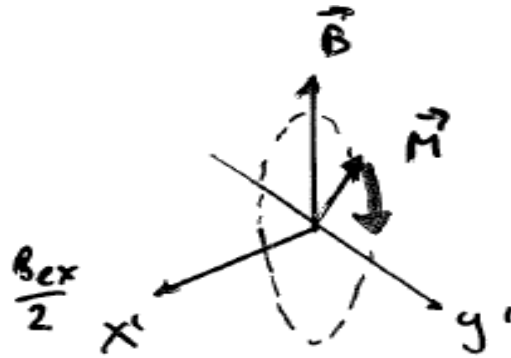
90° excitation pulse:  $\omega' \cdot T = \frac{\pi}{2}$

180° excitation pulse:  $\omega' \cdot T = \pi$

After excitation,  $\vec{M}$  will go through a relaxation process and turn back to its former direction along the  $\vec{B}$ -direction, during the time interval  $T_1$  (Spin-lattice relaxation period). Loss of phase coherence in the  $x'y'$  plane occurs due to spin-spin interaction with the time constant  $T_2^* (< T_1)$ .

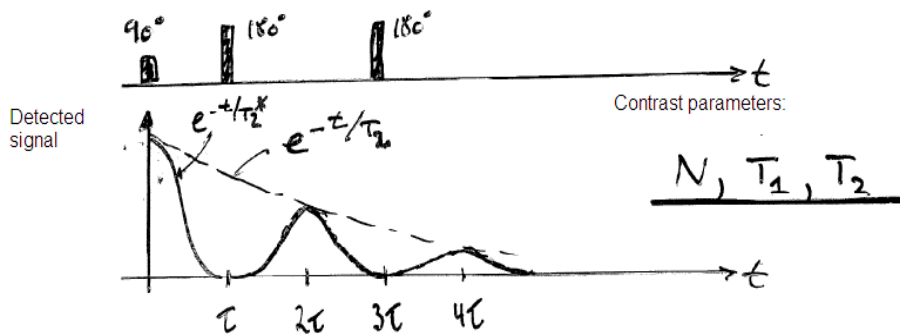
Spin echo (measured by the observer in the rotating co-ordinate system, rotating at the Larmor

frequency).



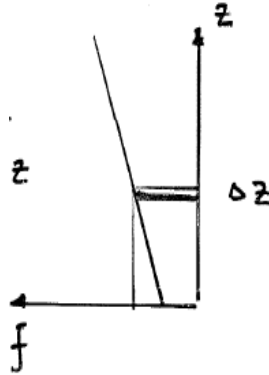
$180^\circ$  precession around  $x'$  due to the excitation field  $\frac{B_{ex}}{2}$ .

Pulse sequence:



## MR tomography (cross-sectional imaging)

Selective excitation of a section by a field gradient ( $B_z$ ) in the  $z$ -direction.



Field:  $\vec{B} = \vec{B}_0 + z\vec{B}_z$

$\Rightarrow f_{ex} = f_{Larmor}$  for a section of thickness  $\Delta z$

Read-out gradient in the  $\phi$ -direction in the cross-sectional plane  $(x, y)$

$\Rightarrow$  The signal represents the sum of the signal for all  $y'$  at each value of  $x'$  in the  $\phi$ -direction.

$\Rightarrow$  Projection imaging and image reconstruction by filtered back-projection.